Power-Constrained Distributed Implementation of SNR-Optimal Collaborative Beamforming in Highly-Scattered Environments

Slim Zaidi, *Student Member, IEEE*, Bouthaina Hmidet, and Sofiène Affes, *Senior Member, IEEE*

Abstract—In this letter, we consider a power-constrained signal-to-noise ratio (SNR)-optimal collaborative beamformer (OCB) design in highly-scattered environments. We show that its weights depend on non-local CSI (NLCSI), thereby hampering its implementation in a distributed fashion. Exploiting the polychromatic (i.e., multi-ray) structure of scattered channels, we propose a novel distributed CB (DCB) design whose weights depends solely on local CSI (LCSI) and prove that it performs nearly as well as its NLCSI-based counterpart. Furthermore, we prove that the proposed LCSI-based DCB outperforms two other distributed-implementation benchmarks: the monochromatic (i.e., single-ray) DCB (M-DCB) whose design ignores the presence of scattering and the bichromatic (i.e., two-ray) DCB (B-DCB), which relies on an efficient polychromatic-channel approximation by two rays when the angular spread is relatively small.

Index Terms—Distributed collaborative beamforming, relaying, MIMO, scattering, device/machine-2-device/machine (D2D/M2M) communications, wireless sensor networks (WSN)s.

I. INTRODUCTION

DUE to its strong potential in increasing link reliability, transmission coverage, and wireless networks capacity, collaborative beamforming (CB) has garnered the attention of the research community [1], [2], [4]–[8]. Depending on their implementation modes, the CB techniques proposed so far could be broadly categorized either as local CSI (LCSI)-based (i.e., distributed) CB, namely the monochromatic DCB (M-DCB) and the bichromatic DCB (B-DCB), or non-local CSI (NLCSI)-based (i.e., non-distributed) CB, namely the optimal CB. When designing M-DCB, authors in [1], [2] ignored scattering present in almost all real-world scenarios but very few ones, still offering both practical and investigation values, in which they have consequently assumed a simple monochromatic (i.e., single-ray) channel. In scattered channels, however, said to be polychromatic (i.e., multi-ray) and characterized by the angular spread (AS) [3]–[7] due to channel mismatch, the performance of M-DCB slightly deteriorates in areas where the AS is small and becomes unsatisfactory when it grows large [4]–[7]. In contrast, B-DCB in [5] which accounts for scattering by an efficient two-ray approximation of the polychromatic channel at relatively low AS not only outperforms M-DCB, but also achieves optimal performance at small to moderate AS values in lightly- to moderately-scattered environments. Nevertheless, its performance substantially deteriorates in highly-scattered environments [5]. OCB which is able to achieve
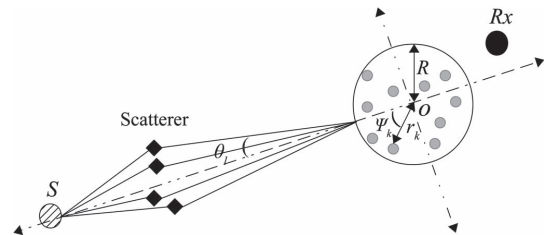
Fig. 1. System model.

optimal performance even in highly-scattered environments is NLCSI-based and cannot be implemented in a truly distributed fashion over a network of independent wireless terminals [6]. Indeed, the latter must estimate and broadcast their own channels at the expense of an overhead that becomes prohibitive for a large number of terminals and/or high Doppler [6], [7]. The aim of this work is then to design a novel DCB implementation that requires a minimum overhead cost and, further, is able to achieve optimal performance for any AS values, thereby pushing farther the frontier of the DCB's real-world applicability range to include highly-scattered environments.

In this letter, we consider a power-constrained OCB design that maximizes, in highly-scattered environments, the received SNR. We verify that its direct implementation is NLCSI-based. Exploiting the polychromatic structure of scattered channels, we propose a novel LCSI-based DCB implementation that requires a minimum overhead cost and, further, performs nearly as well as its NLCSI-based OCB counterpart. Furthermore, we prove that the proposed LCSI-based DCB always outperforms both M-DCB and B-DCB.

II. SYSTEM MODEL

Consider a wireless network comprised of K single-antenna terminals uniformly and independently distributed on the disc $D(O, R)$. A source S and a receiver Rx are located in the same plane containing $D(O, R)$, as illustrated in Fig. 1. Due to high pathloss attenuation, we assume that there is no direct link from S to Rx. Let (r_k, ψ_k) and (A_s, ϕ_s) denote the polar coordinates of the k-th terminal and the source, respectively. The latter is assumed, without loss of generality, to be at $\phi_s = 0$ and to be located relatively far from the terminals, i.e., $A_s \gg R$.

Furthermore, the following assumptions are considered throughout the letter: A1) The backward channel gain $[\mathbf{g}]_k$ from the source to the k-th terminal is polychromatic due to the presence of scattering [3]–[7]. Exploiting the fact that $A_s \gg R$, $[\mathbf{g}]_k$ could be represented as $[\mathbf{g}]_k = \sum_{l=1}^{L} \alpha_l e^{-j\frac{2\pi}{\lambda} r_k \cos(\theta_l - \psi_k)}$ where λ is the wavelength, L is the number of impinging chromatics (i.e., rays), and α_l and θ_l are the l-th chromatic's complex amplitude and angle deviation from ϕ_s, respectively. The α_l, $l = 1, \ldots, L$ and θ_l, $l = 1, \ldots, L$ are i.i.d zero-mean random variables. The α_ls have a variance $1/L$ while the θ_ls have a probability density function (pdf) (i.e., scattering or

angular distribution) $p(\theta)$ and a standard deviation (i.e., angular spread (AS)) σ_θ. All θ_ls and α_ls are mutually independent. A2) The terminals' forward channels to the receiver $[\mathbf{f}]_k$, $k = 1, \ldots, K$ are zero-mean unit-variance circular Gaussian random variables [5]–[8]. A3) The source signal s is narrow-band with unit power while noises at the terminals and the receiver are zero-mean Gaussian random variables with variances σ_v^2 and σ_n^2, respectively [5]–[9]. A4) The k-th terminal is aware of its own coordinates (r_k, ψ_k), its forward channel $[\mathbf{f}]_k$, its backward channel $[\mathbf{g}]_k$, and the wavelength λ while being oblivious to the locations and the forward channels of *all* other terminals in the network [1], [2], [5].

A dual-hop communication, where the k-th terminal multiplies the signal received from S by its weight w_k and forwards it to Rx, is established. The received signal at Rx is given by

$$r = s\mathbf{w}^H\mathbf{h} + \mathbf{w}^H(\mathbf{f} \odot \mathbf{v}) + n, \qquad (1)$$

where $\mathbf{w} \triangleq [w_1 \ldots w_K]$ is the beamforming vector, $\mathbf{h} \triangleq \mathbf{f} \odot \mathbf{g}$ with $\mathbf{f} \triangleq [[\mathbf{f}]_1 \ldots [\mathbf{f}]_K]^T$, $\mathbf{g} \triangleq [[\mathbf{g}]_1 \ldots [\mathbf{g}]_K]^T$, and $\odot$ is the element-wise product, and $\mathbf{v}$ and n are the terminals' noise vector and the receiver noise, respectively. Several CB designs exist in the literature, but we are only concerned herein by the power-Constrained SNR-optimal design [8].

III. POWER-CONSTRAINED SNR-OPTIMAL CB

Let $\mathbf{w}_O$ denote the power-constrained SNR-optimal CB (OCB) which satisfies the following optimization problem:

$$\mathbf{w}_O = \arg \max \xi_\mathbf{w} \quad \text{s.t.} \quad P_T \le P_{\max}, \qquad (2)$$

where, from (1), $\xi_\mathbf{w} = P_{\mathbf{w},s}/P_{\mathbf{w},n}$ is the achieved SNR using $\mathbf{w}$ with $P_{\mathbf{w},s} = |\mathbf{w}^H\mathbf{h}|^2$ is the received power from S, $P_{\mathbf{w},n} = \sigma_v^2\mathbf{w}^H\mathbf{\Lambda}\mathbf{w}+\sigma_n^2$ is the noises' power, $\mathbf{\Lambda} \triangleq \mathrm{diag}\{|[\mathbf{f}]_1|^2 \ldots |[\mathbf{f}]_K|^2\}$, and $P_T = \mathbf{w}^H\mathbf{D}\mathbf{w}$ is the terminals' total transmit power where $\mathbf{D} \triangleq \mathrm{diag}\{|[\mathbf{g}]_1|^2 \ldots |[\mathbf{g}]_K|^2\} + \sigma_v^2\mathbf{I}$. Note that $\mathbf{w}_O$ should satisfy the constraint in (2) with equality.[1] Otherwise, one could find $\epsilon > 1$ such that $\mathbf{w}_\epsilon = \epsilon\mathbf{w}_O$ verifies $P_T = P_{\max}$. In such a case, since $d\xi_{\mathbf{w}_\epsilon}/d\epsilon > 0$ for any $\epsilon > 0$, the SNR achieved by $\mathbf{w}_\epsilon$ would be higher than that achieved by $\mathbf{w}_O$ contradicting thereby the optimality of the latter. It is straightforward to show that the optimal solution of (2) is

$$\mathbf{w}_O = \left(\frac{P_{\max}}{K\eta}\right)^{\frac{1}{2}} \tilde{\mathbf{\Lambda}}^{-1}\mathbf{h}, \qquad (3)$$

where $\eta = \left(\mathbf{h}^H\tilde{\mathbf{\Lambda}}^{-1}\mathbf{D}\tilde{\mathbf{\Lambda}}^{-1}\mathbf{h}\right)/K$ with $\tilde{\mathbf{\Lambda}} = \mathbf{\Lambda} + \beta\mathbf{I}$ and $\beta = \sigma_n^2/(\sigma_v^2 P_{\max})$. Nevertheless, the implementation of OCB according to (3) is NLCSI-based since the computation of its beamforming weight $[\mathbf{w}_O]_k$ at the k-th terminal depends on information unavailable locally, namely $[\mathbf{g}]_k$, $k = 1, \ldots, K$ and $[\mathbf{f}]_k$, $k = 1, \ldots, K$ as well as $P_{\max}/K$ and $\sigma_n^2/P_{\max}$. In order to implement $\mathbf{w}_O$ in the considered network, each terminal should then estimate its backward channel and broadcast it over the network along with its forward channel. This process results in an undesired overhead which becomes prohibitive especially for large K and/or high backward channel's Doppler, resulting thereby in substantial throughput losses [6]. Therefore, OCB is unsuitable for implementation in the network of interest, unless relatively exhaustive overhead exchange over the air

[1] The power budget at each terminal is assumed here greater than $P_{\max}$.

were acceptable or if $\mathbf{w}_O$ were to be implemented in conventional beamforming, i.e., over a unique physical terminal that connects to a K-dimensional distributed antenna system (DAS).

IV. PROPOSED DCB IMPLEMENTATION

In order to reduce the excessively large implementation overhead incurred by the NLCSI-based OCB, we resort to substitute η with a quantity that could be locally computed by all terminals at a negligible overhead cost. This quantity must also well-approximate η to preserve the optimality of the solution in (3). In this letter, we propose to use $\eta_D = \lim_{K\to\infty} \eta$ in lieu of η. First, we show that

$$\eta = \frac{1}{K}\sum_{k=1}^K \frac{|[\mathbf{f}]_k|^2}{\left(|[\mathbf{f}]_k|^2 + \beta\right)^2} \sum_{l=1}^L \sum_{m=1}^L \alpha_l\alpha_m^* e^{j4\pi\sin\left(\frac{\theta_l-\theta_m}{2}\right)z_k}, \qquad (4)$$

where $z_k = (r_k/\lambda)\sin((\theta_l+\theta_m)/2 - \psi_k)$. Using the strong law of large numbers and the fact that r_k, ψ_k and $[\mathbf{f}]_k$ are all mutually statistically independent, we have

$$\eta_D = \lim_{K\to\infty} \eta \quad \xrightarrow{p1} \quad \rho_1 \sum_{l=1}^L \sum_{m=1}^L \alpha_l\alpha_m^*\Delta(\theta_l - \theta_m), \qquad (5)$$

where $\xrightarrow{p1}$ stands for the convergence with probability one, $\rho_1 = \mathrm{E}\left\{|f|^2/(|f|^2 + \beta)^2\right\} = -(1+\beta)e^\beta\mathrm{Ei}(-\beta) - 1$, $\mathrm{Ei}(x)$ is the exponential integral function, and $\Delta(\phi) = \mathrm{E}\left\{e^{j4\pi\sin(\phi/2)z}\right\}$. To derive the closed-form expression of $\Delta(\phi)$, note that we require the z_k's pdf $f_{z_k}(z)$ which is closely related to the terminals' spatial distribution. In this letter, we are only concerned by the main distributions frequently used in the context of collaborative beamforming, i.e., the Uniform and Gaussian distributions. It can be shown that [1], [2]

$$f_{z_k}(z) = \begin{cases} \frac{2\lambda}{R\pi}\sqrt{1 - \left(\frac{\lambda}{R}z\right)^2}, & -\frac{R}{\lambda} \le z \le \frac{R}{\lambda} \quad \text{Uniform} \\ \frac{\lambda}{\sqrt{2\pi}\sigma}e^{-\frac{(\lambda z)^2}{2\sigma^2}}, & -\infty \le z \le \infty \quad \text{Gaussian}, \end{cases} \qquad (6)$$

where σ^2 is the variance of the Gaussian random variables corresponding to the terminals' cartesian coordinates. Using (6) we obtain

$$\Delta(\phi) = \begin{cases} 2\frac{J_1\left(4\pi\frac{R}{\lambda}\sin(\phi/2)\right)}{4\pi\frac{R}{\lambda}\sin(\phi/2)}, & \phi \ne 0 \quad \text{Uniform} \\ 1, & \phi = 0 \\ e^{-8\left(\pi\frac{\sigma}{\lambda}\sin(\phi/2)\right)^2}, & \text{Gaussian}, \end{cases} \qquad (7)$$

where $J_1(x)$ is the first-order Bessel function of the first kind. Substituting η with η_D in (3), we introduce

$$[\mathbf{w}_P]_k = \left(\frac{P_{\max}}{K\eta_D}\right)^{\frac{1}{2}} \frac{[\mathbf{f}]_k[\mathbf{g}]_k}{\left(|[\mathbf{f}]_k|^2 + \beta\right)^2}, \qquad (8)$$

the k-th terminal's beamforming weight of our proposed DCB. From (8), in contrast with $[\mathbf{w}_O]_k$, $[\mathbf{w}_P]_k$ solely depends on the forward and backward channels $[\mathbf{f}]_k$ and $[\mathbf{g}]_k$, respectively, which can be locally estimated. Therefore, according to (8), the proposed beamformer's implementation is LCSI-based and requires only a negligible overhead that does not grow neither with K nor with the Doppler, namely $P_{\max}/K$, $\sigma_n^2/P_{\max}$, and R or σ depending on the terminals' spatial distribution. Consequently, the proposed LCSI-based DCB is much more suitable for a distributed implementation over the considered

network than its NLCSI-based OCB counterpart. Furthermore, we will prove in the sequel that it performs nearly as well as the latter even for a relatively small number of terminals. We will also compare it with two other LCSI-based DCB benchmarks, namely M-DCB and the recently developed B-DCB. The former's design ignores scattering and assumes a monochromatic channel and, hence, its CB solution reduces from (8) to $\mathbf{w}_M = \left(\frac{P_{\max}}{K\rho_1}\right)^{\frac{1}{2}} \tilde{\mathbf{\Lambda}}^{-1}\mathbf{a}(0)$ where $[\mathbf{a}(\theta)]_k = [\mathbf{f}]_k e^{-j(2\pi/\lambda)r_k \cos(\theta - \psi_k)}$. In turn, the B-DCB design whose CB solution reduces from (8) to $\mathbf{w}_{BD} = \left(\frac{P_{\max}}{K\rho_1}\right)^{\frac{1}{2}} \frac{\tilde{\mathbf{\Lambda}}^{-1}(\mathbf{a}(\sigma_\theta) + \mathbf{a}(-\sigma_\theta))}{(1 + \Delta(2\sigma_\theta))}$ relies on a polychromatic channel's approximation by two chromatics at $\pm\sigma_\theta$ when the latter is relatively small.

V. PERFORMANCE ANALYSIS OF THE PROPOSED DCB

Let $\bar{\xi}_{\mathbf{w}} = \mathrm{E}\{P_{\mathbf{w},s}/P_{\mathbf{w},n}\}$ be the achieved average SNR (ASNR) using the CB vector $\mathbf{w}$. Note that the expectation is taken with respect to r_k, ψ_k and $[\mathbf{f}]_k$ for $k = 1, \ldots, K$ and α_l and θ_l for $l = 1, \ldots, L$. Since to the best of our knowledge, $\bar{\xi}_{\mathbf{w}}$ for $\mathbf{w} \in \{\mathbf{w}_P, \mathbf{w}_O, \mathbf{w}_M\}$ is untractable in closed-form thereby hampering its study rigorously, we propose to adopt instead the average-signal-to-average-noise ratio (ASANR) $\tilde{\xi}_{\mathbf{w}} = \mathrm{E}\{P_{\mathbf{w},s}\}/\mathrm{E}\{P_{\mathbf{w},n}\}$ as a performance measure to gauge the proposed DCB against its benchmarks [5]–[7].

A. Proposed DCB vs M-DCB

Following derivation steps similar to those in [5, Appendix A] and exploiting the fact that, according to A1, we have

$$\mathrm{E}\{\alpha_l^* \alpha_m\} = \begin{cases} 0 & l \neq m \\ \frac{1}{L} & l = m, \end{cases} \quad (9)$$

we obtain $\mathrm{E}\{P_{\mathbf{w}_P,s}\} = \frac{P_{\max}}{\rho_1}\left(\rho_2 + (K-1)\rho_3^2\right)$ where $\rho_2 = \mathrm{E}\{|[\mathbf{f}]_k|^4/(|[\mathbf{f}]_k|^2 + \beta)^2\} = 1 + \beta + \beta(2+\beta)e^\beta \mathrm{Ei}(-\beta)$ and $\rho_3 = \mathrm{E}\{|[\mathbf{f}]_k|^2/(|[\mathbf{f}]_k|^2 + \beta)\} = 1 + \beta e^\beta \mathrm{Ei}(-\beta)$. Furthermore, to derive $\mathrm{E}\{P_{\mathbf{w}_P,n}\}$, one must first take the expectation only over the r_ks, ψ_ks and $[\mathbf{f}]_k$s yielding to $\mathrm{E}_{r_k,\psi_k,[\mathbf{f}]_k}\{P_{\mathbf{w}_P,n}\} = \sigma_v^2 \frac{P_{\max}\rho_2 \sum_{l,m=1}^L \alpha_l\alpha_m^* \Delta(\theta_l - \theta_m)}{\eta_D} + \sigma_n^2 = \sigma_v^2 \frac{P_{\max}\rho_2}{\rho_1} + \sigma_n^2$. It directly follows from the latter results that the achieved ASANR using the proposed DCB is

$$\tilde{\xi}_{\mathbf{w}_P} = \frac{\rho_2 + (K-1)\rho_3^2}{\sigma_v^2(\rho_2 + \beta\rho_1)}. \quad (10)$$

As can be observed from (10), $\tilde{\xi}_{\mathbf{w}_P}$ linearly increases with the number of terminals K. More importantly, from the latter result, $\tilde{\xi}_{\mathbf{w}_P}$ does not depend on the AS σ_θ meaning that the proposed DCB's performance is not affected by the scattering phenomenon even in highly-scattered environments where σ_θ is large. Now, let us focus on the achieved ASANR $\tilde{\xi}_{\mathbf{w}_M}$ using M-DCB. Following the same approach above, one can prove that

$$\tilde{\xi}_{\mathbf{w}_M} = \frac{\rho_2 + (K-1)\rho_3^2 \int_\Theta p(\theta)\Delta^2(\theta)d\theta}{\sigma_v^2(\rho_2 + \beta\rho_1)}, \quad (11)$$

where Θ is the span of the pdf $p(\theta)$ over which the integral is calculated.[2] Since $\Delta(0) = 1$ regardless of the terminals' spatial distribution, it follows from (10) and (11) that

[2]In the Gaussian and Uniform distribution cases, $\Theta = [-\inf, +\inf]$ and $\Theta = [-\sqrt{3}\sigma_\theta, +\sqrt{3}\sigma_\theta]$, respectively.

when there is no scattering (i.e., $\sigma_\theta = 0$), $\tilde{\xi}_{\mathbf{w}_M} = \tilde{\xi}_{\mathbf{w}_P}$. In such a case, indeed, $\mathbf{w}_P = \mathbf{w}_M \sum_{l=1} \alpha_l / \sqrt{\sum_{l=1}\alpha_l \sum_{m=1}\alpha_m^*}$ and, hence, $P_{\mathbf{w}_P,s} = P_{\mathbf{w}_M,s} \sum_{l=1}\alpha_l \sum_{m=1}\alpha_m^*$. Since according to (9) $\mathrm{E}\{\sum_{l=1}\alpha_l \sum_{m=1}\alpha_m^*\} = 1$, we have $\mathrm{E}\{P_{\mathbf{w}_P,s}\} = \mathrm{E}\{P_{\mathbf{w}_M,s}\}$. Furthermore, it is straightforward to show that $P_{\mathbf{w}_P,n} = P_{\mathbf{w}_M,n}$ when $\sigma_\theta = 0$ and, therefore, M-DCB achieves the same ASANR as the proposed DCB when there is no scattering. This is in fact expected since the assumption of monochromatic channel made when designing the monochromatic solution is valid in such a case. Nevertheless, assuming that the terminals's spatial distribution and the scattering distribution $p(\theta)$ are both Uniform, it can be shown for relatively small AS that [10]

$$\tilde{\xi}_{\mathbf{w}_M} \simeq \frac{\rho_2 + (K-1)\rho_3^2 \, _3F_4\left(\frac{1}{2}, 2, \frac{3}{2}; \frac{3}{2}, 2, 2, 3, -12\pi^2\left(\frac{R}{\lambda}\right)^2\sigma_\theta^2\right)}{\sigma_v^2(\rho_2 + \beta\rho_1)}, \quad (12)$$

where $_3F_4\left(\frac{1}{2}, 2, \frac{3}{2}; \frac{3}{2}, 2, 2, 3, -12\pi^2(R/\lambda)^2x^2\right)$ is a decreasing function of x whose peak is reached at 0 known as hypergeometric function. It can be inferred from (12), that the ASANR achieved by the M-DCB decreases when the AS σ_θ and/or R/λ increases. This is in contrast with the proposed DCB whose ASANR remains constant for any σ_θ and R/λ. Therefore, the proposed DCB is more robust against scattering than M-DCB whose design ignores the presence of scattering.

B. Proposed DCB vs OCB

As $P_{\mathbf{w}_O,s}$ and $P_{\mathbf{w}_O,n}$ are a very complicated functions of several random valuables, it turns out that it is impossible to derive the ASANR $\tilde{\xi}_{\mathbf{w}_O}$ in closed-form. However, a very interesting result could be obtained for large K. Indeed, one can show that

$$\lim_{K\to\infty} \frac{\tilde{\xi}_{\mathbf{w}_O}}{\tilde{\xi}_{\mathbf{w}_P}} = \frac{(\rho_2 + \beta\rho_1)\mathrm{E}\left\{\frac{1}{\eta_D}\left(\lim_{K\to\infty}\frac{\mathbf{h}^H\tilde{\mathbf{\Lambda}}^{-1}\mathbf{h}}{K}\right)^2\right\}}{\rho_3^2\left(\mathrm{E}\left\{\frac{1}{\eta_D}\lim_{K\to\infty}\frac{\mathbf{h}^H\tilde{\mathbf{\Lambda}}^{-1}\mathbf{\Lambda}\tilde{\mathbf{\Lambda}}^{-1}\mathbf{h}}{K}\right\} + \beta\right)}$$
$$\xrightarrow{p1} \frac{\frac{(\rho_2+\beta\rho_1)}{\rho_1}\mathrm{E}\left\{\left(\sum_{l,m=1}^L \alpha_l\alpha_m^* \Delta(\theta_l - \theta_m)\right)\right\}}{\frac{\rho_2}{\rho_1} + \beta} = 1, \quad (13)$$

where the second line exploits (9) and the law of large numbers by which we can prove that $\lim_{K\to\infty}\mathbf{h}^H\tilde{\mathbf{\Lambda}}^{-1}\mathbf{h}/K = \rho_3 \sum_{l,m=1}^L \alpha_l\alpha_m^* \Delta(\theta_l - \theta_m)$ and $\lim_{K\to\infty}\mathbf{h}^H\tilde{\mathbf{\Lambda}}^{-1}\mathbf{\Lambda}\tilde{\mathbf{\Lambda}}^{-1}\mathbf{h}/K = \rho_2 \sum_{l,m=1}^L \alpha_l\alpha_m^* \Delta(\theta_l - \theta_m)$. For large K, the latter result proves that the proposed LCSI-based DCB is able to achieve the same ASANR as the NLCSI-based OCB and, therefore, is able to reach optimality for any AS value. This further proves the efficiency of the proposed DCB.

Using the same method as in (13), one can easily show that $\lim_{K\to\infty} \tilde{\xi}_{\mathbf{w}}/\bar{\xi}_{\mathbf{w}} \xrightarrow{p1} 1$ for $\mathbf{w} \in \{\mathbf{w}_P, \mathbf{w}_O, \mathbf{w}_M\}$. Therefore, all the above results hold also for the ASNR as K grows large.

Please note that analytical comparison of the proposed DCB with B-DCB is not disclosed here due to space limitation. However, it has been shown in [5] that the latter's performance is optimal for small to moderate AS while it severely deteriorates when the AS is large. In such a case, indeed, the channels' two-ray approximation over which relies B-DCB is no longer valid. Consequently, the proposed DCB is more robust to scattering than B-DCB as illustrated by simulations in Fig. 3.
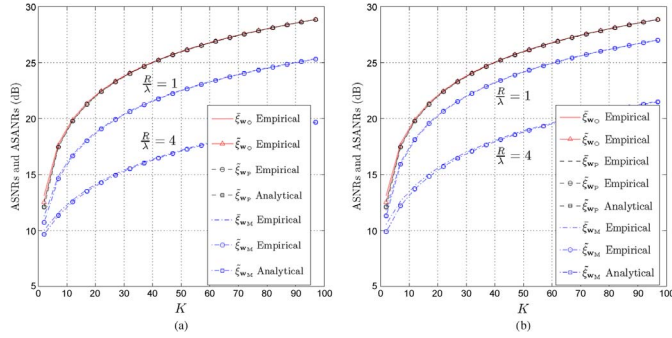
Fig. 2. The empirical ASNRs and ASANRs achieved by $\mathbf{w} \in \{\mathbf{w}_O, \mathbf{w}_P, \mathbf{w}_M\}$ as well as the analytical ASANRs achieved by $\mathbf{w}_P$ and $\mathbf{w}_M$ versus K for $\sigma_\theta = 20$ (deg) and $R/\lambda = 1, 4$ when the terminals' spatial distribution is (a): Uniform and (b): Gaussian.

Fig. 3. The empirical ASNRs and ASANRs achieved by $\mathbf{w} \in \{\mathbf{w}_O, \mathbf{w}_{BD}, \mathbf{w}_P, \mathbf{w}_M\}$ as well as the analytical ASANRs achieved by $\mathbf{w}_P$ and $\mathbf{w}_M$ versus σ_θ for $K = 20$ and $R/\lambda = 1$ when the terminals' spatial distribution is (a): Uniform and (b): Gaussian.

VI. SIMULATION RESULTS

All the empirical average quantities, in this section, are obtained by averaging over 10^6 random realizations of all random variables. In all simulations, the number of rays or chromatics is $L = 10$ and the noises' powers σ_n^2 and σ_v^2 are 10 dB below the source transmit power $p_s = 1$ power unit on a relative scale. We also assume that the scattering distribution is uniform (i.e., $p(\theta) = 1/(2\sqrt{3}\sigma_\theta)$) and that α_ls are circular Gaussian random variables. For fair comparisons between the Uniform and Gaussian spatial distributions, we choose $\sigma = R/3$ to guarantee in the Gaussian distribution case that more than 99% of terminals are located in $D(O, R)$.

Fig. 2 plots the empirical ASNRs and ASANRs achieved by $\mathbf{w} \in \{\mathbf{w}_O, \mathbf{w}_P, \mathbf{w}_M\}$ as well as the analytical ASANRs achieved by $\mathbf{w}_P$ and $\mathbf{w}_M$ versus K for $\sigma_\theta = 20$ (deg) and $R/\lambda = 1, 4$. The terminals' spatial distribution is assumed to be Uniform in Fig. 2(a) and Gaussian in Fig. 2(b). From these figures, we confirm that the analytical $\tilde{\xi}_{\mathbf{w}_P}$ and $\tilde{\xi}_{\mathbf{w}_M}$ match perfectly their empirical counterparts. As can be observed from these figures, the proposed DCB outperforms M-DCB in terms of achieved ASANR. Furthermore, the ASANR gain achieved using the proposed DCB instead of the latter substantially increases when R/λ grows large. Moreover, from Fig. 2(a) and (b), the achieved ASANR using the proposed LCSI-based DCB fits perfectly with that achieved using NLCSI-based OCB, which is unsuitable for a distributed implementation, when K is in the range of 20 while it looses only a fraction of a dB when K is in the range of 5. This proves that the proposed DCB is able to reach optimality when K is large enough. It can be also verified from these figures that $\tilde{\xi}_{\mathbf{w}_P}$ and $\tilde{\xi}_{\mathbf{w}_B}$ perfectly match $\bar{\xi}_{\mathbf{w}_P}$ and $\bar{\xi}_{\mathbf{w}_M}$, respectively, for $K = 20$. All these observations corroborate the theoretical results obtained in Section V.
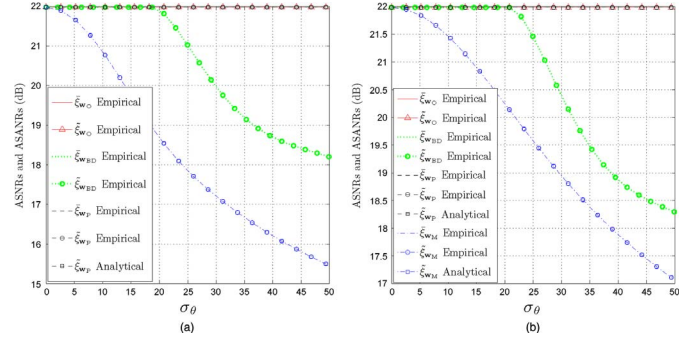
Fig. 3 displays the empirical ASNRs and ASANRs achieved by $\mathbf{w} \in \{\mathbf{w}_O, \mathbf{w}_{BD}, \mathbf{w}_P, \mathbf{w}_M\}$ as well as the analytical ASANRs achieved by $\mathbf{w}_P$ and $\mathbf{w}_M$ versus the AS for $K = 20$ and $R/\lambda = 1$. It can be observed from this figure that the ASANR achieved by M-DCB decreases with the AS while that achieved by the proposed beamformer remains constant. This corroborates again the theoretical results obtained in Section V. Furthermore, we observe from Fig. 3 that B-DCB achieves the same ASNR as the proposed DCB when the AS is relatively small such as in lightly- to moderately-scattered environments. Nevertheless, in highly-scattered environments where the AS is large (i.e., $\sigma_\theta \geq 20$ deg), the proposed DCB outperforms B-DCB whose performance further deteriorates as σ_θ grows large. This is

expected since the two-ray channel approximation made when designing B-DCB is only valid for small σ_θ. Moreover, it can be noticed from Fig. 3(a) and (b), that the ASNR gain achieved using the proposed DCB instead of M-DCB and B-DCB can reach until about 6.5 (dB) and 4 (dB), respectively. From these figures, we also observe that the curves of $\bar{\xi}_{\mathbf{w}_P}$ and $\bar{\xi}_{\mathbf{w}_O}$ are indistinguishable. As pointed out above, this is due to the fact that both OCB and the proposed DCB constantly reach optimality.

VII. CONCLUSION

In this letter, we considered a power-constrained SNR-optimal CB design. We verified that the direct implementation of this CB design is NLCSI-based. Exploiting, the polychromatic structure of scattered channels, we proposed a novel LCSI-based DCB implementation that requires a minimum overhead cost and, further, performs nearly as well as its NLCSI-based OCB counterpart. Furthermore, we proved that the proposed DCB implementation always outperforms both M-DCB and B-DCB.

REFERENCES

[1] H. Ochiai, P. Mitran, H. V. Poor, and V. Tarokh, "Collaborative beamforming for distributed wireless ad hoc sensor networks," *IEEE Trans. Signal Process.*, vol. 53, no. 11, pp. 4110–4124, Nov. 2005.

[2] M. F. A. Ahmed and S. A. Vorobyov, "Collaborative beamforming for wireless sensor networks with Gaussian distributed sensor nodes," *IEEE Trans. Wireless Commun.*, vol. 8, no. 2, pp. 638–643, Feb. 2009.

[3] M. Bengtsson and B. Ottersten, "Low-complexity estimators for distributed sources," *IEEE Trans. Signal Process.*, vol. 48, no. 2, pp. 2185–2194, Aug. 2000.

[4] A. Amar, "The effect of local scattering on the gain and beamwidth of a collaborative beampattern for wireless sensor networks," *IEEE Trans. Wireless Commun.*, vol. 9, no. 9, pp. 2730–2736, Sep. 2010.

[5] S. Zaidi and S. Affes "Distributed collaborative beamforming in the presence of angular scattering," *IEEE Trans. Commun.*, vol. 62, no. 5, pp. 1668–1680, May 2014.

[6] S. Zaidi and S. Affes, "SNR and throughput analysis of distributed collaborative beamforming in locally-scattered environments," *J. Wireless Commun. Mobile Comput.*, vol. 12, no. 18, pp. 1620–1633, Dec. 2012.

[7] S. Zaidi and S. Affes, "Analysis of collaborative beamforming designs in real-world environments," in *Proc. IEEE WCNC*, Shanghai, China, Apr. 7–10, 2013, pp. 3518–3523.

[8] V. Havary-Nassab, S. Shahbazpanahi, A. Grami, and Z.-Q. Luo, "Distributed beamforming for relay networks based on second-order statistics of the channel state information," *IEEE Trans. Signal Process.*, vol. 56, no. 9, pp. 4306–4316, Sep. 2008.

[9] G. Zheng, K.-K. Wong, A. Paulraj, and B. Ottersten, "Collaborative-relay beamforming with perfect CSI: Optimum and distributed implementations," *IEEE Signal Process. Lett.*, vol. 16, no. 4, pp. 257–260, Apr. 2009.

[10] I. S. Gradshteyn and I. M. Ryzhik, *Table of Integrals, Series and Products*, 7th ed. San Diego, CA, USA: Academic, 2007.